Eur. Phys. J. A **20**, 435–441 (2004)
DOI 10.1140/epja/i2003-10175-2

THE EUROPEAN PHYSICAL JOURNAL A

The ^{16}O(e, e′pp)^{14}C reaction to discrete final states

J. Ryckebusch[a] and W. Van Nespen

Department of Subatomic and Radiation Physics, Ghent University, Proeftuinstraat 86, B-9000 Gent, Belgium

Received: 3 September 2003 / Revised version: 2 December 2003 /
Published online: 18 June 2004 –
Communicated by Th. Walcher

Abstract. Differential cross-sections for exclusive $^{16}\mathrm{O}(e,e'pp)^{14}\mathrm{C}$ processes are computed within a distorted-wave framework which includes central short-range correlations and intermediate Δ^+ excitations. The cross-sections are compared to high-resolution data from the MAMI facility at Mainz for a central energy and momentum transfer of $\langle\omega\rangle = 215$ MeV and $\langle q\rangle = 316$ MeV, respectively. A fair agreement between the numerical calculations and data is reached when using spectroscopic information extracted from a $^{15}\mathrm{N}(d,{}^3\mathrm{He})^{14}\mathrm{C}$ experiment. The comparison between the calculations and the data provides additional evidence that short-range correlations exclusively affect nucleon pairs with a small center-of-mass momentum residing in a relative S state.

PACS. 24.10.-i Nuclear-reaction models and methods – 21.60.-n Nuclear-structure models and methods – 25.30.Fj Inelastic electron scattering to continuum

1 Introduction

The presence of short-range correlations (SRC) in nuclei is intimately connected to the finite extension of the nucleons. Over the years, a variety of experiments have been hunting for signatures of these SRC. Major progress has been made with experiments involving electrons as initial probe. More in particular, the study of double-coincidence $A(e,e'p)$ processes has considerably improved our knowledge about the dynamics of protons embedded in a nuclear medium. The major share of the $A(e,e'p)$ experiments has been conducted in quasi-elastic kinematics, whereby the experimental parameters are adjusted so as to provide a relation between the measured differential cross-sections and the momentum distribution of the hit proton. The momentum distribution provides us with knowledge about the probability that a nucleon in a well-defined orbit has a given value of momentum. After correcting for final-state interaction (FSI) effects, the momentum dependence of the extracted momentum distributions nicely reproduced the predictions of non-relativistic and relativistic nuclear mean-field approaches up to momenta approaching the Fermi momentum $k_{\mathrm{F}} \approx 250$ MeV. At the same time, from the absolute magnitude of the measured cross-sections it could be inferred that when integrating over the mean-field part of the momentum distributions one ends up with a value which is about 70% of what could be expected on the basis of the amount of protons populating the target nucleus. This depletion is attributed to the presence of sizable short- and long-range correlations in atomic nuclei of which one believes that they exhibit a rather complex radial, spin, isospin and tensor behaviour. An economical way of parameterizing nucleon-nucleon correlations is the introduction of correlation operators with a strength determined by radial-dependent correlation functions [1]. The determination of these correlation functions is pivotal in the study of many correlated systems and the nucleus represents no exception in this matter. The nuclear central correlation function, which corresponds with the unity correlation operator, is believed to have similar characteristics as the two-particle correlation functions (or, radial distribution functions) of molecules in liquids [2]. Indeed, when moving with a nucleon in the nucleus, its finite extension will induce a reduced probability of finding another nucleon over distances of the order of its radius R_p and an increased probability at distances slightly larger than R_p. The radial distribution function for molecules in liquids shows a similar fluctuating behaviour and can be understood through the molecule-molecule repulsion extending over distances of the size of a molecule. Usually, this repulsion is modeled with the aid of a Lennard-Jones potential [2].

Experimentally determining the correlation function turns out to be challenging. It is expected that triple-coincidence reactions of the $A(e,e'pp)$ type could improve our knowledge about the dynamics of nucleon pairs and help in mapping the radial dependence of the central correlation function. Pioneering experimental work

[a] e-mail: jan.ryckebusch@UGent.be

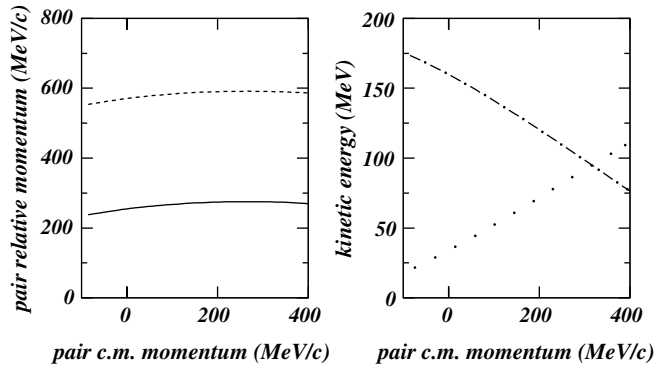

Fig. 1. The kinetic energies (right panel) and pair relative momenta $p_{\rm rel} = \mid \frac{\boldsymbol{k}_1 - \boldsymbol{k}_2}{2} \pm \frac{\boldsymbol{q}}{2} \mid$ (left panel) as a function of the pair c.m. momentum for the ^{16}O$(e,e'pp)^{14}$C$(0^+,$g.s.) reaction in super-parallel kinematics at $\langle\omega\rangle = 215$ MeV and $\langle q\rangle = 316$ MeV. In the left panel, the dashed (solid) line refers to the "+" ("−") case of eq. (1). In the right panel, the dot-dashed (dotted) curve refers to the nucleon parallel (anti-parallel) to the momentum transfer $\boldsymbol{q}$.

was done at the AMPS electron accelerator in Amsterdam [3–5]. Building on this experience, in the final years of operation of this facility, high-quality data could be collected for the ^{3}He$(e,e'pp)n$ [6] and ^{16}O$(e,e'pp)^{14}$C process [7]. Complementary measurements on the ^{12}C [8] and ^{16}O$(e,e'pp)$ [9,10] reaction have been performed at the 850 MeV electron accelerator in Mainz. These two-proton knockout measurements have sparked off a lot of theoretical activity of which some of the more recent ones include the work reported in refs. [11–13]. An ambitious two-proton knockout calculation aiming at consistently computing the long- and short-range correlations in ^{16}O, in combination with a treatment of final-state interaction effects, has been presented in ref. [14]. Recently, this model has been extended to include the mutual interactions between the two ejected protons [11].

The first high-resolution $A(e,e'pp)$ data which could clearly separate the individual states in the final nucleus became recently available [9,10]. The data were collected by the A1 Collaboration with a unique three-spectrometer setup at the MAMI facility in Mainz [15]. An initial electron beam energy of 855 MeV and an ^{16}O target was used. The two ejected protons, with momenta $\boldsymbol{k}_1$ and $\boldsymbol{k}_2$, were detected parallel and anti-parallel to the momentum transfer, a peculiar situation which is known as "super-parallel kinematics". The energy and momentum transfer was kept constant at a central value of $\langle\omega\rangle = 215$ MeV and $\langle q\rangle = 316$ MeV. Data were collected in a pair missing momentum $P \equiv \mid \boldsymbol{k}_1 + \boldsymbol{k}_2 - \boldsymbol{q} \mid$ range of $-100 \leq P \leq 400$ MeV/c. In a naive spectator model the quantity P corresponds with the center-of-mass (c.m.) momentum of the diproton at the instant of its interaction with the virtual photon. The quantity $p_{\rm rel}$ is defined according to

$$p_{\rm rel} = \left| \frac{\boldsymbol{k}_1 - \boldsymbol{k}_2}{2} \pm \frac{\boldsymbol{q}}{2} \right| . \qquad (1)$$

In an ideal world with vanishing final-state interactions, $p_{\rm rel}$ would denote the relative momentum of the active proton pair before its interaction with the photon, with the $-$ $(+)$ sign in eq. (1) referring to the situation whereby the virtual photon hits proton "1" ("2"). Figure 1 displays the range in kinetic energies and pair relative momenta which is covered in the ^{16}O$(e,e'pp)^{14}$C experiment of refs. [9,10] for which calculations will be presented in this paper. The curves refer to the kinematics corresponding with the ground-state transition. As we will restrict ourselves to relatively low excitation energies in ^{14}C, the variation in kinetic energies and relative pair momenta is similar for all transitions which will be considered here. A strong variation in the proton kinetic energies with the pair c.m. momentum is observed, whereas the pair relative momentum is fairly constant.

2 The model for electro-induced two-proton knockout

The numerical ^{16}O$(e,e'pp)$ calculations presented here, are performed in a non-relativistic distorted-wave model outlined in refs. [16,17]. It is based on a partial-wave expansion for the A-nucleon final state in terms of two-particle two-hole ($2p$-$2h$) eigenstates of the Hartree-Fock Hamiltonian. A similar approach has been adopted in ref. [13]. In this work, the one-body Hartree-Fock Hamiltonian is derived self-consistently starting from an effective nucleon-nucleon force of the Skyrme type. The adopted partial-wave expansion for the final state reads

$$\begin{aligned} |\Psi_f\rangle \equiv & \left|\Psi_f^{(A-2)}(E_x, J_R M_R); \boldsymbol{k}_1 m_{s_1}; \boldsymbol{k}_2 m_{s_2}\right\rangle \\ = & \sum_{l_1 m_{l_1} j_1 m_1} \sum_{l_2 m_{l_2} j_2 m_2} (4\pi)^2 i^{l_1+l_2} \frac{\pi}{2m_p\sqrt{k_1 k_2}} \\ & \times e^{i(\delta_{l_1}+\sigma_{l_1}+\delta_{l_2}+\sigma_{l_2})} \times Y^*_{l_1 m_{l_1}}(\Omega_1) Y^*_{l_2 m_{l_2}}(\Omega_2) \\ & \times \left\langle l_1 m_{l_1} \frac{1}{2} m_{s_1} \;\middle|\; j_1 m_1 \right\rangle \left\langle l_2 m_{l_2} \frac{1}{2} m_{s_2} \;\middle|\; j_2 m_2 \right\rangle \\ & \times \left|\Psi_f^{(A-2)}(E_x, J_R M_R)\right\rangle \\ & \times |(p_1(E_1 l_1 j_1 m_1)\, p_2(E_2 l_2 j_2 m_2))\rangle \ , \end{aligned} \qquad (2)$$

where m_p is the proton mass and the particle (or, continuum) eigenstates p_i of the mean-field Hamiltonian are characterized by the quantum numbers $(E_i l_i j_i m_i)$. The energy E_i of the ejectile is determined by its momentum $\boldsymbol{k}_i$. The central and Coulomb phase shifts for the protons 1 and 2 are denoted by $(\delta_{l_1},\, \sigma_{l_1})$ and $(\delta_{l_2},\, \sigma_{l_2})$. Further, $\left|\Psi_f^{(A-2)}(E_x, J_R M_R)\right\rangle$ specifies the quantum numbers of the state in which the residual $A-2$ nucleus is left. In our approach, the initial and final A-nucleon states are orthogonal and anti-symmetrized. The first property implies that the overlap between the wave function for the ground state of the target nucleus and the wave functions of eq. (2) vanishes exactly. This is of particular importance in view of the fact that in computing cross-sections for

triple-coincidence reactions characterized by small cross-sections, great care must be exercised to avoid all possible sources of spurious contributions entering the overlap matrix elements.

As will become clear in the forthcoming discussions, an important ingredient of the calculations are the two-hole overlap amplitudes $X^{E_x}_{hh'}$ which determine the Two-nucleon Overlap Functions (TOFs) between the ground state of the target nucleus and each of the probed states in the residual nucleus. These coefficients play an analogous role as the "spectroscopic factors" in $A(e,e'p)$ processes and are frequently referred to as $n \rightarrow n-2$ cfp coefficients. At this point, it is worth stressing that in the analysis of single-proton knockout reactions of the $A(e,e'p)$ type, the spectroscopic factors are usually treated as parameters which are extraced by normalizing the computed to the measured differential cross-sections.

In a direct two-proton knockout process, solely the "two-hole" components in the final state will be excited. Accordingly, that piece of the final $A-2$ wave function which can be excited in a direct two-proton knockout reaction can be written in terms of an expansion of the form

$$\begin{aligned}\left|\Psi_f^{(A-2)}(E_x, J_R M_R)\right\rangle &= \sum_{hh'} X^{E_x}_{hh'} \left|\left(h^{-1}h'^{-1}\right) J_R\ M_R\right\rangle \\ &= \sum_{hh'} X^{E_x}_{hh'} \sum_{m_h m_{h'}} \frac{1}{\sqrt{1+\delta_{hh'}}} \\ &\quad \times \langle j_h m_h j_{h'} m_{h'} \mid J_R M_R\rangle \\ &\quad \times (-1)^{j_h+m_h+j_{h'}+m_{h'}} \\ &\quad \times c_{h-m_h} c_{h'-m_{h'}} \left|\Psi_0\right\rangle\ , \end{aligned} \tag{3}$$

where $|\Psi_0\rangle$ is the ground state of the target nucleus which serves as the natural choice for the reference state. In the ^{16}O$(e,e'pp)$ reaction model calculations presented here, the overlap amplitudes $X^{E_x}_{hh'}$ are treated as input parameters. In determining their magnitudes we will be guided by empirical information gathered in transfer reactions with hadronic probes. An alternative and ambitious approach, adopted *e.g.* by the Pavia group, is to use the TOFs (or, equivalently, the spectroscopic information) predicted by advanced shell-model calculations [12,14]. Despite the enormous efforts directed at calculating the TOFs, it turns out that the most sophisticated two-hole spectral function calculations for ^{16}O still miss some key features of the low-lying states in ^{14}C [18].

Qualitatively, the missing energy spectra extracted from the analysis of the Mainz high-resolution ^{16}O$(e,e'pp)$ experiment bear a strong resemblance with those obtained in a ^{15}N$(d,{}^3$He$)^{14}$C [19] and ^{16}O$(^6$Li,^{8}B$)^{14}$C [20] measurement. In essence, the ground state (0^+), a doublet of 2^+ states (respectively, at $E_x = 7.01$ and 8.32 MeV), a 1^+ state at $E_x = 11.31$ MeV and a 0^+ state at $E_x = 9.75$ MeV are populated. As a matter of fact, we will exploit this similarity to guide our choices with respect to the spectroscopic information for the two-nucleon overlap functions entering the numerical calculations.

In essence, the eightfold $(e,e'pp)$ differential cross-sections are computed starting from the transition amplitude

$$J^\mu(\boldsymbol{q}) = \int \mathrm{d}\boldsymbol{r} \left\langle \Psi_f \left| e^{i\boldsymbol{q}\cdot\boldsymbol{r}} J^\mu(\boldsymbol{r}) \right| \Psi_0 \right\rangle\ , \tag{4}$$

where $\boldsymbol{q}$ is the momentum transfer induced by the virtual photon, and J^μ the nuclear current operator. The operator J^μ considered here is the sum of the Δ-isobar current operator, and an operator which is the product of the one-body charge- and current-density $J^\mu_{[1]}(\boldsymbol{r})$ and a central correlation function $g(r_{12} \equiv \mid \boldsymbol{r}_1 - \boldsymbol{r}_2 \mid)$

$$\left(J^\mu_{[1]}(\boldsymbol{r}_1) + J^\mu_{[1]}(\boldsymbol{r}_2)\right) g\left(r_{12}\right) + g^\dagger\left(r_{12}\right) \left(J^\mu_{[1]}(\boldsymbol{r}_1) + J^\mu_{[1]}(\boldsymbol{r}_2)\right). \tag{5}$$

In this current operator, the $g(r_{12})$ term accounts for the effect of SRC in the pair wave function at the time that it was hit by the virtual photon and belongs to the class of initial-state correlations. The $g^\dagger(r_{12})$ term, on the other hand, is part of the class of final-state correlations and implements the effect of SRC on the wave function for the two ejected protons. In order to guarantee the Hermiticity of the above current operator (5), the inital- and final-state short-range correlations are modeled with the aid of the same correlation function. The central correlation function $g(r_{12})$ expresses how strongly two nucleons, which are a distance r_{12} apart, are correlated. In the absence of nucleon-nucleon correlations beyond those already implemented in the independent-nucleon picture, this contribution would simply vanish. A plethora of parameterizations for $g(r)$ can be found in the literature. They range from those that have a hard core extending over more than 1 fm to those with a relatively soft core and sizable probability to find two protons at the same position. Our numerical results are obtained with the correlation function of ref. [21] which categorizes somewhere in between these two extreme classes. The correlation function of ref. [21] was earlier found to provide a favorable agreement with the ^{12}C$(e,e'pp)$ measurements of ref. [8] and the ^{16}O$(e,e'pp)$ data reported in ref. [7]. The Δ-current operator used in this work has an energy- and medium-dependent Δ width. Its detailed form can be found in ref. [22].

3 Results and discussion

We start our discussion of the ^{16}O$(e,e'pp)$ differential cross-sections with the 1^+ state at $E_x = 11.31$ MeV. In most nuclear-structure calculations, the two-proton overlap amplitudes for this particular state are dominated by the $\left|\left(1p_{3/2}\right)^{-1}\left(1p_{1/2}\right)^{-1}; 1^+\right\rangle$ two-hole configuration. As we use realistic single-particle wave functions obtained through solving the Hartree-Fock Hamiltonian, an exact separation into the relative $\boldsymbol{r}_{12} = \boldsymbol{r}_1 - \boldsymbol{r}_2$ and c.m. $\boldsymbol{R} = \frac{\boldsymbol{r}_1+\boldsymbol{r}_2}{2}$ coordinate is not possible in our approach. The well-known Moshinsky transformation for a harmonic-oscillator basis can however serve as a guide to identify the dominant relative and c.m. quantum numbers of the

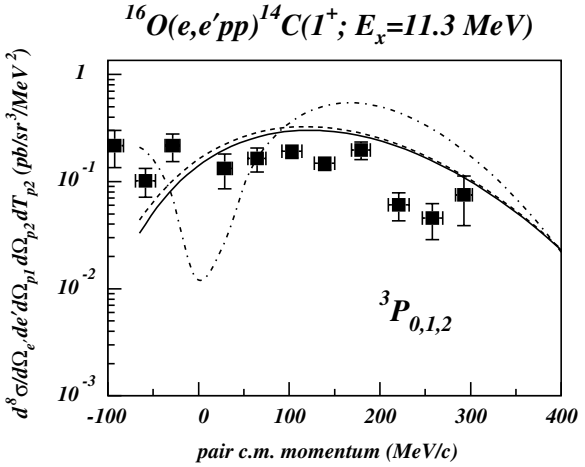

Fig. 2. The eightfold differential cross-section for the $^{16}\mathrm{O}(e,e'pp)^{14}\mathrm{C}(1^+, E_x = 11.31\,\mathrm{MeV})$ reaction as a function of the pair c.m. momentum. The dashed curve shows the results of the distorted-wave calculations that include only the intermediate Δ excitation. The solid (dot-dashed) curve is the result of a distorted-wave (plane-wave) calculation that accounts for both intermediate Δ and central short-range correlations. The data are from refs. [9] and [10].

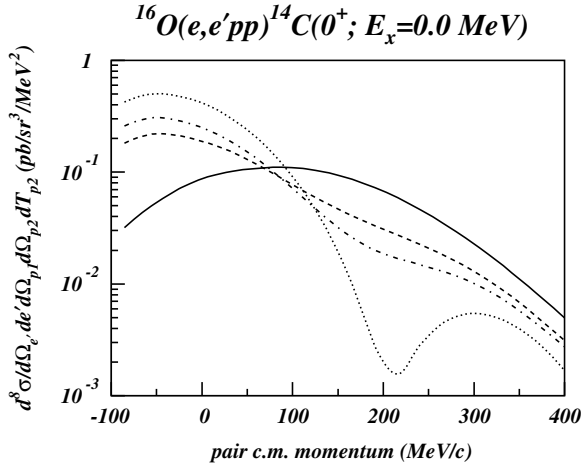

Fig. 3. Calculated differential cross-sections for the $^{16}\mathrm{O}(e,e'pp)^{14}\mathrm{C}(0^+, E_x = 0\,\mathrm{MeV})$ reaction using various sets of two-proton overlap amplitudes. All curves are obtained in a distorted-wave approximation and account for central short-range correlations and intermediate Δ excitation. The calculations use the two-proton overlap amplitudes (m, n) from ref. [25] (solid curve), ref. [24] (dot-dashed curve), ref. [23] (dashed curve) and ref. [26] (dotted curve). The corresponding values for (m, n) are listed in table 1.

Table 1. Two-hole overlap amplitudes for the $^{16}\mathrm{O} \rightarrow {}^{14}\mathrm{C}$ ground-state transition.

	Ref. [23]	Ref. [24]	Ref. [25]	Ref. [26]
m	0.97	0.91	0.76	0.576
n	0.24	0.41	−0.65	0.818

diprotons for a specific transition. Indeed, the quantum numbers of the final state impose strong restrictions on the possible combinations for the relative and c.m. angular momentum of the active diproton. For the $\left|(1p)^{-2}; 1^+\right\rangle$ configuration only the combination of $L = 1$ c.m. and P-wave relative wave functions is allowed. In what follows, we will denote the c.m. angular momentum with L.

The plane-wave $^{16}\mathrm{O}(e,e'pp)^{14}\mathrm{C}(E_x = 11.31\,\mathrm{MeV})$ predictions shown in fig. 2 clearly exhibit this $L = 1$ behaviour. The distortions which the struck protons undergo through the presence of the other target nucleons, fill in the dip in the P-wave pair c.m. momentum distribution about $P \approx 0$. This peculiar feature is also observed in the data. A striking feature of the calculations displayed in fig. 2 is that the Δ contribution is by far the dominant one, while central short-range correlations are only marginally contributing. The distorted-wave model provides a reasonable description of the data. The curves displayed in fig. 2 use an overlap amplitude $X_{hh'}^{E_x=11.31\,\mathrm{MeV}}$ of 1 for the sole component $\left|\left(1p_{3/2}\right)^{-1}\left(1p_{1/2}\right)^{-1}; 1^+\right\rangle$. This number is about 30% larger than the value of 0.76 quoted in ref. [23].

We proceed with discussing the results for the ground-state transition. In contrast to the situation for the 1^+ state, at least two two-hole configurations have been frequently quoted as major contributors to a two-proton transfer process. As a matter of fact, in the spirit of eq. (3) one can write that the relevant components in the ground state of $^{14}\mathrm{C}$ are

$$\left|0^+; E_x = 0\,\mathrm{MeV}\right\rangle = m\left|\left(1p_{1/2}\right)^{-2}; 0^+\right\rangle + n\left|\left(1p_{3/2}\right)^{-2}; 0^+\right\rangle . \quad (6)$$

The precise values of m and n are subject to discussion, though. Table 1 summarizes some of the combinations of values for the two-hole overlap amplitudes m and n that can be found in the literature. Additional sets can be found in tables II and III of ref. [26]. For the sake of clarity the overlap amplitudes contained in table 1 were normalized by putting $m^2 + n^2 = 1$.

The sensitivity of the computed $^{16}\mathrm{O}(e,e'pp)^{14}\mathrm{C}(J^\pi = 0^+, E_x = 0\,\mathrm{MeV})$ differential cross-sections to the choices made with respect to the magnitude of the overlap amplitudes is displayed in fig. 3 containing predictions for each set contained in table 1. The solid line, which corresponds with overlap amplitudes that are obtained from fitting inelastic $M1$ form factors for the $^{14}\mathrm{N}(e,e')(J^\pi = 0^+, T = 1, E_x = 2.313\,\mathrm{MeV})$ transition [25], exhibits a c.m. momentum dependence which is completely out of line from the other three curves. The $\left|(1p)^{-2}; 0^+\right\rangle$ configuration gives rise to relative and c.m. wave functions corresponding with relative $^1S_0$ in combination with $L = 0$ and relative $^3P_1$ combined with $L = 1$.

The results of the NIKHEF $^{16}\mathrm{O}(e,e'pp)^{14}\mathrm{C}(0^+)$ experiments [5,7] provide strong evidence for the presence of a strong $L = 0$ component, thereby excluding the solid curve in fig. 3. It is worth remarking that the overlap amplitudes corresponding with the solid curve stem from a fit to the $M1$ inelastic $^{14}\mathrm{N}(e,e')$ form factor that is not

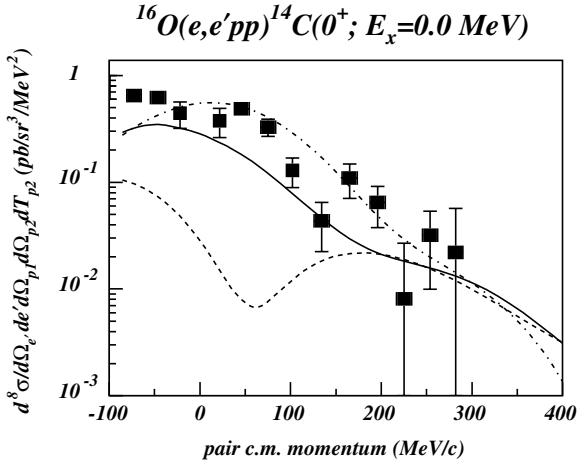

Fig. 4. The eightfold differential cross-section for the ^{16}O$(e,e'pp)^{14}$C$(0^+, E_x = 0\,\mathrm{MeV})$ reaction as a function of the pair c.m. momentum. The dashed curve shows the results of the distorted-wave calculations that include only the intermediate Δ excitation. The solid (dot-dashed) curve is the result of a distorted-wave (plane-wave) calculation that accounts for both intermediate Δ and central short-range correlations. The data are from refs. [9] and [10].

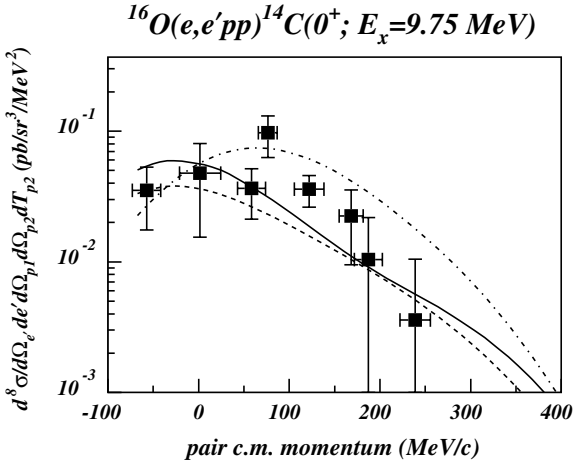

Fig. 5. As in fig. 4 but now for the excitation of the 0^+ state at an excitation energy of 9.75 MeV. The data are from refs. [9] and [10].

particularly sensitive to the $L = 0$ component. The other three curves in fig. 3 correspond with a relative contribution of the $(1p_{1/2})^{-2}$ and $(1p_{3/2})^{-2}$ components that is gradually changing. The larger the contribution from $(1p_{3/2})^{-2}$, the larger the $L = 0$ component and the smaller the $L = 1$ component.

Figure 4 displays a comparison of the recently obtained ^{16}O$(e,e'pp)^{14}$C$(0^+, E_x = 0\,\mathrm{MeV})$ data and our reaction model calculations using the two-hole overlap amplitudes of ref. [24]. The distorted-wave calculations including short-range correlations reproduce the missing-momentum dependence well, while underestimating the data by roughly a factor of two over the whole momentum range. We wish to stress that with the two-hole overlap amplitudes (m, n) from ref. [24], the presented model produced also a reasonable agreement with the ^{16}O$(e,e'pp)^{14}$C$(0^+, E_x = 0\,\mathrm{MeV})$ cross-sections measured at the AMPS facility [7]. These overlap amplitudes compared also favorably with the ^{15}N$(d,{}^3\mathrm{He})^{14}$C$(0^+, \mathrm{g.s.})$ measurements reported in ref. [19]. An interesting observation from fig. 4 is that the distorted-wave calculation ignoring central short-range correlations, underestimates the data at low pair missing momenta by several factors. At high pair missing momenta, where the $(L = 1)$-wave can be expected to dominate, the calculations neglecting the central short-range correlations move closer to the data. In any case, without inclusion of central short-range correlations, neither the shape nor the magnitude of the data for the ground-state transition can be reproduced. We interpret this as strong evidence for short-range correlations for proton pairs residing in relative $^1S_0$ states. At the same time, and equally important, central short-range correlations appear to affect exclusively proton pairs in relative S and c.m. $L = 0$ states.

The superior resolution at the unique MAMI three-spectrometer setup made determining the differential cross-sections for a weakly excited 0^+ state at $E_x = 9.75$ MeV feasible. It is tempting to interpret this state as the "orthogonal" partner of the ground-state. Shell-model calculations, however, predict that the "orthogonal partner" of the ground state is located at a substantially larger excitation energy (respectively, $E_x = 16.32$ MeV in the calculations of ref. [24] and 12.00 MeV in the calculations of ref. [23]). Using the overlap amplitudes quoted in ref. [24] we obtain a differential cross-section which overshoots the data by several factors over the complete pair c.m. momentum range. This suggests that the 9.75 MeV state is not the "orthogonal" partner of the ground state and can at most carry a fraction of the corresponding two-hole strength. Indeed, assuming that about 17% of the two-hole strength contained in the wave function of ref. [24]

$$\left|0_2^+\right\rangle = +0.41 \left|\left(1p_{1/2}\right)^{-2}; 0^+\right\rangle - 0.91 \left|\left(1p_{3/2}\right)^{-2}; 0^+\right\rangle , \quad (7)$$

is carried by the 9.75 MeV state, we obtain the results displayed in fig. 5. It is worth stressing that also the ^{15}N$(d,{}^3\mathrm{He})^{14}$C measurements reported in ref. [19] do not provide evidence for a sizable population of a 0^+ state for $E_x \approx 10$ MeV.

The nuclear-structure calculations of refs. [24] and [23] both assign the following structure:

$$\left|2^+\right\rangle = +0.976 \left|\left(1p_{3/2}\right)^{-1}\left(1p_{1/2}\right)^{-1}; 2^+\right\rangle + 0.212 \left|\left(1p_{3/2}\right)^{-2}; 2^+\right\rangle , \quad (8)$$

to the lowest 2^+ state in ^{14}C. In the analysis of the transfer reaction ^{15}N$(d,{}^3\mathrm{He})^{14}$C measurement reported in ref. [19], it was found that the low-lying 2^+ strength is fragmented over at least three states. In the same paper, a careful

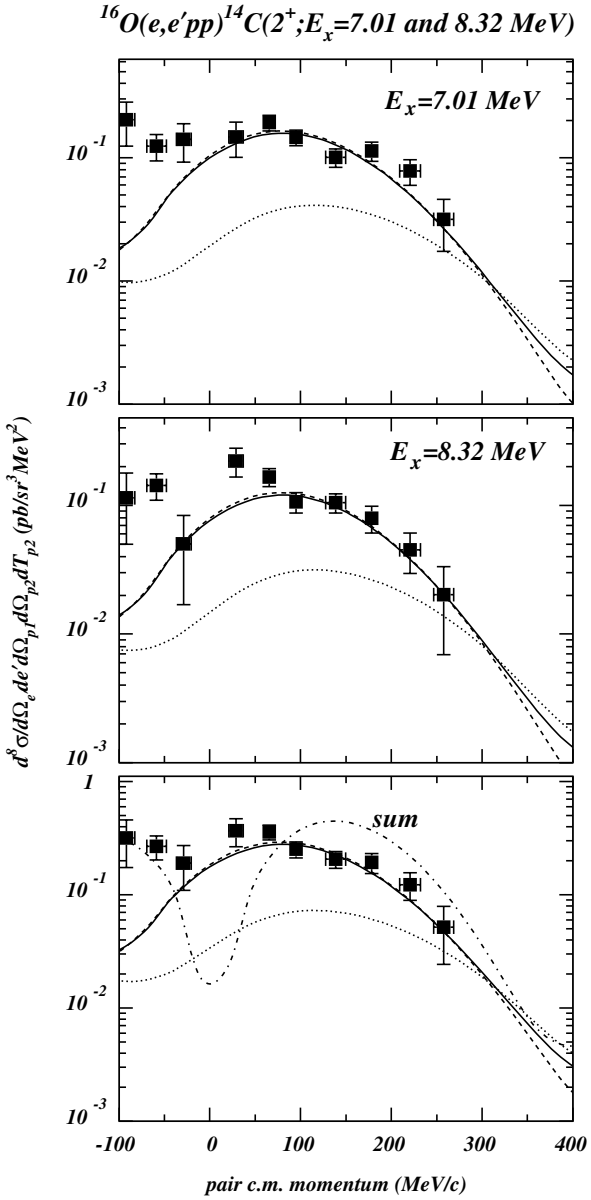

Fig. 6. The eightfold differential cross-section for the ^{16}O$(e,e'pp)^{14}$C$(2^+, E_x = 7.01$ and 8.32 MeV) reaction as a function of the pair c.m. momentum. The dashed curve shows the results of the distorted-wave calculations that include only the intermediate Δ excitation. The solid (dot-dashed) curve is the result of a distorted-wave (plane-wave) calculation that accounts for both intermediate Δ and central short-range correlations. The dotted line omits the core excitations of the $(1s)^2(1p)^4(1d)^2$ type from the full calculations. The data are from refs. [9] and [10].

analysis of the data led to the conclusion that *"whereas the $J^\pi = 0^+$ and 1^+, $T = 1$ states of mass 14 are rather pure $(1p)^{-2}$ states, the 2^+, $T = 1$ states are STRONGLY mixed with core excitations of the $(2s_{1/2}, 1d)^2$ type"*.

The dotted curves in fig. 6 are obtained with the overlap amplitudes contained in eq. (8). For the fragmentation of the strength over the different physical 2^+ states we adopt the values as they were obtained in the aforementioned analysis of ^{15}N$(d, ^3$He$)^{14}$C measurements (*i.e.*, 47% and 36% for the 7.01 and 8.32 MeV state in the doublet). It is clear that when including solely $(1p)^{-2}$ two-hole overlap amplitudes our distorted-wave calculations badly fail in predicting the shape and magnitude of ^{16}O$(e,e'pp)^{14}$C differential cross-sections. A similar result has been obtained with the Pavia $A(e,e'pp)$ model [9]. These failures are probably not so surprising in the light of the findings for the 2^+ transitions in ^{15}N$(d, ^3$He$)^{14}$C measurements [19].

We have taken up the aforementioned suggestion based on an analysis of ^{15}N$(d, ^3$He$)^{14}$C hadron reactions, that important core components may contribute for the 2^+ excitation. After including core polarizations of the $(1s)^2(1p)^4(1d)^2$ type in the target ground-state wave function, which amounts to modifying the $|\Psi_0\rangle$ wave functions of eq. (3) into

$$|\Psi_0\rangle = \sqrt{1-\beta^2}\,\big|(1s)^2\,(1p)^6\big\rangle + \beta\,\big|(1s)^2\,(1p)^4(1d_{5/2})^2\big\rangle\,, \qquad (9)$$

we find the solid curves in fig. 6. The least one can say is that core polarizations have a large impact on the calculated cross-sections for electro-induced two-proton knockout to the 2^+ state. After including the core polarization effects, a reasonable description of the data is reached. For the curves of fig. 6, the $(1s)^2(1p)^4(1d)^2$ core polarization was implemented with an amplitude $\beta = 0.4$, which is a value suggested by the shell-model calculations of ref. [27].

Our predictions for the cross-sections tend to systematically underestimate the data at negative values of the c.m. momentum P. As can be appreciated from inspecting the right panel of fig. 1, negative values of P correspond with an asymmetric situation with an extremely slow forward-going proton. For these slow-moving protons, it cannot be excluded that multiple-scattering contributions, not included in the presented calculation, gain in relative importance.

4 Summary

We have computed the eightfold ^{16}O$(e,e'pp)$ differential cross-sections in a distorted-wave model adopting a direct reaction process. Two-nucleon photoabsorption mechanisms involving intermediate Δ creation and central short-range correlations have been implemented. In non-relativistic approaches, as the one adopted here, meson exchange currents do not contribute to two-proton knockout reactions. In general, the Δ-isobar current is at the origin of the major fraction of the electro-induced two-proton knockout strength, thereby confirming the conclusions drawn in earlier investigations [8]. The effect of central short-range correlations becomes clearly visible for the peculiar case that a diproton remaining in a relative S state can additionally be guaranteed to have a small c.m. momentum. Such conditions can be studied in the ^{16}O(g.s.)$(e,e'pp)^{14}$C(g.s.) reaction. At high c.m. momenta, the differential cross-section for this transition is

indeed dominated by the Δ-isobar current, the short-range correlations providing marginal amounts of strength. At low c.m. momenta, the opposite is true. In line with the observations made in hadronic transfer reactions, a proper description of the excitation of the 2^+ states in ^{14}C requires a strong mixing of the ^{16}O ground state with long-range core polarization components. The presented investigations illustrate that besides questions related to the description of final-state interaction effects and the implementation of two-body currents, an analysis of $A(e, e'pp)$ reactions is highly sensitive to the spectroscopic information. Indeed, unlike in the exclusive $A(e, e'p)$ case, where one can usually identify one dominant single-hole component for a particular transition, the two-nucleon knockout process to individual states is often the result of several strongly interfering two-hole overlap amplitudes. For the latter quantities, which refer to the long-range dynamics of nuclei, widely varying predictions can be found in the literature. With respect to the magnitudes for the two-hole overlap amplitudes, we adopt a heuristic view and found that the values which did fairly well in explaining hadron transfer reactions, also provide a reasonable description of the ^{16}O$(e, e'pp)$ angular cross-sections to individual states. Often, a consistent description of the short-range (central correlation function) and the long-range (two-hole overlap amplitudes) dynamics of nuclei is considered essential to arrive at a rigorous, coherent theoretical picture of the $A(e, e'pp)$ reaction. The effect of SRC being confined to proton pairs in a relative S state, the Pauli principle decouples the effect of short-range and long-range dynamics to a large degree. Indeed, for the results presented here the expected synergy between the short- and long-range dynamics is solely applicable to the ^{16}O(g.s.)$(e, e'pp)^{14}$C(g.s.) reaction at low pair c.m. momenta. The ^{16}O(g.s.)$(e, e'pp)^{14}$C(g.s.) reaction at high pair c.m. momentum and the transitions to the other low-lying states in ^{14}C are rather dominated by the synergy of Δ degrees of freedom and the long-range dynamics of the nuclei involved.

References

1. Steven C. Pieper, R.B. Wiringa, V.R. Phandharipande, Phys. Rev. C **46**, 1741 (1992).
2. Charles E. Hecht, *Statistical Thermodynamics and Kinetical Theory* (Dover Publications, Mineolo, New York, 1990).
3. A. Zondervan *et al.*, Nucl. Phys. A **587**, 697 (1995).
4. L.J.H.M. Kester *et al.*, Phys. Rev. Lett. **74**, 1712 (1995).
5. G. Onderwater *et al.*, Phys. Rev. Lett. **81**, 2213 (1998).
6. D.L. Groep *et al.*, Phys. Rev. C **63**, 014005 (2001).
7. R. Starink *et al.*, Phys. Lett. B **474**, 33 (2000).
8. K.I. Blomqvist *et al.*, Phys. Lett. B **421**, 71 (1998).
9. G. Rosner, Prog. Part. Nucl. Phys. **44**, 99 (2000).
10. Marco Kahrau, PhD Thesis, *Untersuchung von Nukleon-Nukleon Korrelationen mit Hilfe der Reaktion* ^{16}O$(e, e'pp)^{14}C$ *in super-paralleler Kinematik*, (Johannes Gutenberg-Universität, Mainz, 1999). URL: `http://wwwa1.kph.uni-mainz.de/A1/publications/doctor/kahrau.ps.gz`.
11. M. Schwamb, S. Boffi, C. Giusti, F.D. Pacati, Eur. Phys. J. A **17**, 7 (2003).
12. D.N. Kadrev, M.V. Ivanov, A.N. Antonov, C. Giusti, F.D. Pacati, Phys. Rev. C **68**, 014167 (2003).
13. Marta Anguiano, Giampaolo Có, Antonio M. Lallena, J. Phys. G **29**, 1119 (2003).
14. C. Giusti, F.D. Pacati, K. Allaart, W.J.W. Geurts, W.H. Dickhoff, H. Müther, Phys. Rev. C **57**, 1691 (1998).
15. The A1 Collaboration at the MAMI electron accelator in Mainz: `http://wwwa1.kph.uni-mainz.de/A1/`.
16. J. Ryckebusch, M. Vanderhaeghen, L. Machenil, M. Waroquier, Nucl. Phys. A **568**, 828 (1994).
17. J. Ryckebusch, V. Van der Sluys, K. Heyde, H. Holvoet, W. Van Nespen, M. Waroquier, M. Vanderhaeghen, Nucl. Phys. A **624**, 581 (1997).
18. C. Barbieri, W.H. Dickhoff, Phys. Rev. C **65**, 064313 (2002).
19. G. Kaschl, G. Mairle, H. Mackh, D. Hartwig, U. Schwinn, Nucl. Phys. A **178**, 275 (1971).
20. R.B. Weisenmiller, N.A. Jelley, K.H. Wilcox, G.J. Zozniak, Joseph Cerny, Phys. Rev. C **13**, 1330 (1976).
21. C.C. Gearhart, PhD Thesis, (Washington University, St-Louis, 1994), unpublished.
22. Jan Ryckebusch, Dimitri Debruyne, Wim Van Nespen, Stijn Janssen, Phys. Rev. C **60**, 034604 (1999).
23. W.J.W. Geurts, K. Allaart, W.H. Dickhoff, H. Müther, Phys. Rev. C **54**, 1144 (1996).
24. S. Cohen, D. Kurath, Nucl. Phys. A **141**, 145 (1970).
25. N. Ensslin, W. Bertozzi, S. Kowalkski, C.P. Sargent, W. Turchinetz, C.F. Williamson, S. Fivozinsky, J. Lightbody, S. Penner, Phys. Rev. C **9**, 1704 (1974).
26. R.L. Huffman, J. Dubach, R.S. Hicks, M.A. Plum, Phys. Rev. C **35**, 1 (1987).
27. A.P. Zuker, Phys. Rev. Lett. **23**, 983 (1969).